The concept of the terahertz generator based on an array of double-walled carbon nanotubes with a direct current pump

Sergey A. Afanas'ev,[a]* Aleksei S. Kadochkin,[a] Dmitry G. Sannikov,[a,b] Andrei A. Fotiadi[a,c]

[a] Ulyanovsk State University, 42 Leo Tolstoy str., Ulyanovsk, Russia
[b] Kotelnikov Institute of Radioengineering and Electronics of the Russian Academy of Sciences, Ulyanovsk Branch, 48/2 Goncharov Str., Ulyanovsk, Russia
[c] Electromagnetism and Telecommunication Department, University of Mons, Mons, B-7000, Belgium
*asa_rpe@mail.ru

ABSTRACT

A technique enabling the generation of THz radiation using an ordered array of double-walled carbon nanotubes (DWCNTs) pumped by a direct electric current is proposed. The initial excitation of surface plasmon polaritons (SPPs) in the DWCNTs is performed by two laser beams with slightly different frequencies. The amplification of exited slow SPPs (with a phase velocity down to ~10^6 m/s) is provided by a drift current flowing through the DWCNTs. The DWCNTs with SPPs act as sources of THz radiation and emit coherent electromagnetic waves into free space. The proposed model of a carbon nanotube generator may be useful for the development of compact sources of coherent THz radiation.

Keywords: double-walled carbon nanotubes, surface plasmon polaritons, laser excitation, drift current pumping, terahertz radiation

INTRODUCTION

To date, several technologies for the production of ordered arrays of carbon nanotubes (CNTs) with controlled parameters have been established [1–5]. Carbon nanotubes have a number of unique properties: individual CNTs (and their arrays) are capable of conducting currents of high density (over 10 A/mm^2 in direct current (DC) and 10^9 A/mm^2 in pulsed modes) [6,7], CNTs support propagation of drift currents with a velocity of about 10^6 m/s [8,9]; at the same time CNTs support the propagation of ultraslow surface plasmon polaritons (SPPs) with a long mean free path [10–14].

The huge values of the wavenumber associated with ultraslow surface plasmon polaritons (SPPs) (therefore with the large SPP effective refractive index) prevent their excitation using standard optical techniques. We propose as the possible solution in this case preliminary excitation of SPPs in the ordered CNT arrays by one or two laser beams with close optical frequencies. The beating of two laser beams with detuned frequencies is widely used for THz generation [15–19].

The main idea of the proposed THz source is the recently reported in Refs. [20–24] effect of amplification of SPPs by a drift current arising when the phase matching condition is met. This amplification can not only compensate the SPP attenuation but exceed the value of ohmic losses by several orders of magnitude [24].

The inhomogeneity of the gain spectrum arising due to inhomogeneity of the CNT array could prevent the implementation of this idea. Different CNTs support slow SPP modes at different frequencies, so their simultaneous excitation could lead to noise generation. Routine way to enhance the generation conditions is to use an external resonator providing a high Q-factor for modes of a particular frequency. In this work, we propose to use the optical field created by two laser sources with a small frequency detuning as a factor leading to the matching of surface wave oscillations in CNTs. The proposed concept of the coherent THz generator includes the following components: the preliminary optical excitation of SPP modes in the CNT array by laser beams; the amplification of slow SPP modes by a drift current flowing through the CNTs; the generation of coherent THz radiation by an array of optically synchronized CNTs with DC electric current pumping [19].

Terahertz Photonics III, edited by Mona Jarrahi, Sascha Preu, Dmitry Turchinovich,
Proc. of SPIE Vol. 12994, 129940L · © 2024 SPIE ·
0277-786X · doi: 10.1117/12.3017240

DESCRIPTION OF THE STRUCTURE

We consider a two-dimensional ordered array of identical double-walled carbon nanotubes (DWCNTs) of external radius a and length L, located parallel to each other by the same distance d (Figure 1). Two laser beams with close frequencies ω_1, ω_2 ($\omega_2 < \omega_1$) and with wave numbers $k_{1,2} = \omega_{1,2}/c$ are incident on this structure at angles φ_1 and φ_2 to the axis x (in normal to the axes of the tubes). When the conditions of phase matching are met, the SPP generation occurs at the difference frequency $\omega = \omega_1 - \omega_2$. The wavelength of the first laser beam corresponds to the second harmonic of an erbium-doped fiber laser operating at $\lambda_1 \sim 1.55$ μm, and the wavelength of the second beam $\lambda_2 = 2\pi c / \omega_2$ is tunable over the range sufficient to generate SPP at the difference frequency ω of several THz.

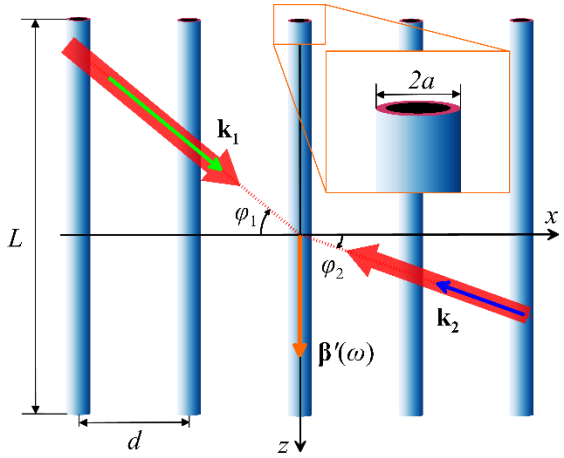

Figure 1. Scheme of the incidence of two laser beams on an array of DWCNTs.

In the projection onto the z axis, the phase-matching condition for two incident laser beams is written as

$$k_1(\omega_1)\sin\varphi_1 + k_2(\omega_2)\sin\varphi_2 = \beta'(\omega), \tag{1}$$

where β' is the wave number of the SPP excited in CNTs. The plasmon frequency in Eq. (1) is up-limited by the value $\omega_{\max}$, which is the solution of the equation

$$\omega_{\max} + \beta'(\omega_{\max})c = \omega_1(1+\sin\varphi_1). \tag{2}$$

In the range of frequencies, where $\beta'(\omega)$ is approximated by a linear dependence with a constant phase velocity $V_{\text{ph}} = \omega/\beta'$, $\omega_{\max}$ is found using Eq. (2) as

$$\omega_{\max} = \omega_1 \frac{(1+\sin\varphi_1)}{1+c/V_{\text{ph}}}. \tag{3}$$

The highest value of $\omega_{\max}$ is achieved when the first laser beam is directed along the CNTs in the array ($\varphi_1 = 90^\circ$).

To simulate the plasmonic properties of doped CNTs with a large diameter (more than several nanometers) the conductivity calculated for graphene can be used [25–27]:

$$\sigma(\omega) = \sigma^{inter}(\omega) + \sigma^{intra}(\omega), \qquad \sigma^{intra}(\omega) = \frac{2ie^2 k_B T}{\pi\hbar^2\left(\omega + i\tau^{-1}\right)} \ln\left[2\cosh\left(\frac{\mu}{2k_B T}\right)\right],$$
$$\sigma^{inter}(\omega) = \frac{e^2}{4\pi\hbar}\left[\frac{\pi}{2} + \arctan\left(\frac{\hbar\omega - 2\mu}{2k_B T}\right) - \frac{i}{2}\ln\frac{(\hbar\omega + 2\mu)^2}{(\hbar\omega - 2\mu)^2 + (2k_B T)^2}\right]. \tag{4}$$

In Eq. (4), σ^{inter} and σ^{intra} are the contribution of inter- and intraband transitions, e is the electron charge, $\hbar$ is the Planck constant, k_B is the Boltzmann constant, T is the temperature, μ is the graphene chemical potential, τ is the average lifetime of carriers. For numerical calculations, the following parameters are taken: T = 300 K, μ = 0.2 eV, and $2\pi\hbar/\tau = 0.1$ meV [28]. The used value of chemical potential of doped graphene corresponds to the surface concentration of carriers $n_s = 4 \cdot 10^{12}$ cm^{-2} [29].

At the frequencies of some tens of THz, the intraband term σ^{intra} dominates in Eq. (1). In the calculations we use modified Drude-type formula:

$$\sigma(\omega,\beta) = \frac{ie^2\mu\,\omega}{\pi\hbar^2\left[\omega\left(\omega + i\tau^{-1}\right) - V_F^2\beta^2/2\right]}, \qquad (5)$$

where the denominator contains a term that takes into account the spatial dispersion in the electron gas associated with the finiteness of the perturbation propagation velocity [14,30]. In Eq. (5) V_F is the Fermi velocity, β is the complex propagation constant of SPPs.

NUMERICAL RESULTS AND DISCUSSION

Figure 2 shows the dispersion curves $\beta'(\omega)$ and $\beta''(\omega)$ for the three lowest-order SPP modes in DWCNT, abstained using numerical calculation software. The calculations are performed for the array of parallel DWCNTs with the external radius of a = 5 nm, distance between walls of 0.34 nm and grating period of $d = 3a$ = 15 nm. We assume that the length of DWCNTs $L >> a, d$. One can see from Figure 2 that in the frequency range up to 22 THz, there is only one propagating mode (curves 1). It is the fundamental mode with the field possessing no azimuthal dependence. The relationship between the frequency and the propagation constant for this SPP mode is close to linear.

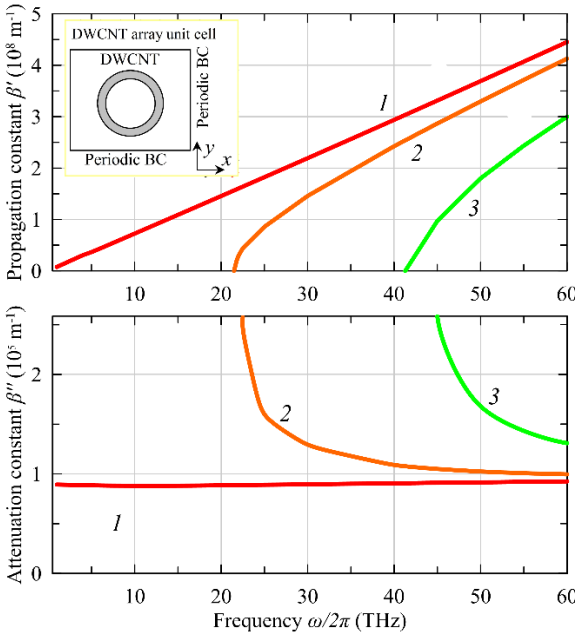

Figure 2. Dispersion dependences for the first three interlayer SPP modes (numbers 1, 2 and 3) in the array of DWCNTs.

A specific feature of the interlayer SPP mode is the presence of a longitudinal component of the electric field E_z. We have found that the parameter $\eta = |E_z|^2 / |E|^2$ ($|E|$ is the modulus of the electric field strength of the SPPs) is about 0.6 at frequencies of several THz making the SPP interaction with the drift current efficient.

In the frequency range from 5 to 25 THz the phase velocity V_{ph} takes the value of about $0.85 \cdot 10^6$ m/s, which provides the deceleration coefficient (effective refractive index) c / V_{ph} of approximately 350. Such a strong deceleration allows the SPPs to interact with a drift current flowing through the DWCNT possessing a charge carrier velocity $V_0 \sim (0.5–1) \cdot 10^6$ m/s [8,9].

For the numerical analysis of Eq. (1), we use the characteristics of the fundamental interlayer SPP mode with a constant phase velocity of $V_{ph} = 8.5 \cdot 10^5$ m/s. The Eq. (3) gives the maximum frequency of the excited SPP $\omega_{max} \approx 0.0057 \omega_1$. For incident radiation with a wavelength of 0.775 μm and angle of incidence $\varphi_1 = 90^\circ$ we get ω_{max} = 2.19 THz. Figure 3 shows the angle of incidence of the second beam φ_2 versus frequency ω of the SPPs excited in the DWCNT array for three values of angle φ_1. One can see that for each frequency ω in the range $\omega < \omega_{max}$ there are two directions of the second beam propagation, which are symmetrically directed with respect to the *z* axis.

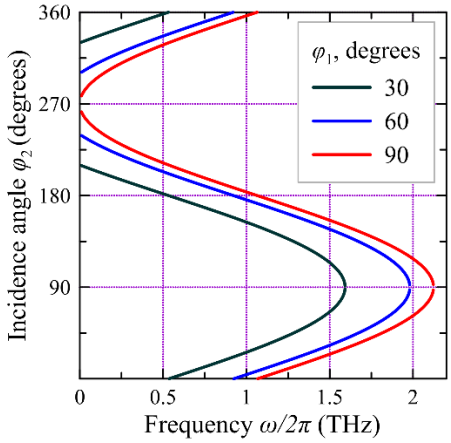

Figure 3. Frequency dependences of the angle of incidence of the second laser beam φ_2 corresponding to the phase-matching condition Eq. (1) at φ_1 = 30°, 60°, and 90°.

To describe the interaction of slow SPPs with DC current and calculate the energy transfer between the electromagnetic wave and the electronic subsystem of the DWCNT, we use the approach based on the application of working principles of traveling wave tube amplifiers [31]. The basics of this approach are outlined in the papers [19,21,23,24,32–34].

This approach uses the equations describing the interaction between of the current and the electromagnetic wave in the waveguide obtained in a perturbative approach. Under the assumption that the current and electric field vary along the DWCNT in proportion to exp(−*iGz*), where *G* is the wave number of the harmonic perturbation, the condition for the compatibility of the system of equations leads to the dispersion equation

$$(\omega - GV_{ph})\left((\omega - GV_0)^2 - \omega_q^2\right) = C^3\omega^3, \qquad (6)$$

where $\omega_q = \chi \cdot \omega_p$ is the reduced plasma frequency depending on the waveguide geometry (for the numerical calculations we take an estimation $\chi \approx 0.35$ from Ref. [35]), $C = \left(eR_c J_0 / 2mV_0 V_{ph}\right)^{1/3}$, $R_c = |E_z|^2 / 2\beta'^2 P$, $P = \frac{1}{2}\varepsilon_0 V_{gr} \int |\mathbf{E}|^2 \, dS$ is a power carried by an electromagnetic wave, V_{gr} is the group velocity of SPPs, J_0 is the current intensity in a single DWCNT, *e* and *m* are the charge and the mass of charge carriers in the nanotube, ε_0 is the permittivity of the vacuum. The Eq. (6) is

resolved by one real root (lines 3 in Figure 4) and two complex conjugated roots (lines 1 and 2 in Figure 4). According to the calculations performed with the help of COMSOL Multiphysics software, the increment $\alpha = \mathrm{Im}(G) > 0$ can get values of ~10^8 m^{-1} that significantly exceeds the values of ohmic losses in the DWCNT ($|\beta''| \sim 10^5$ m^{-1}).

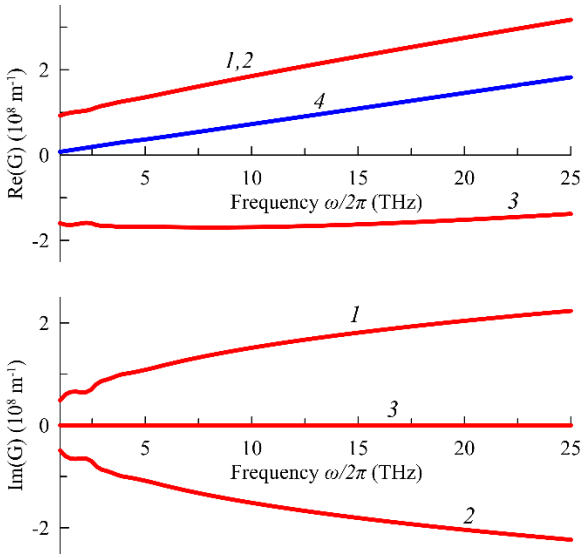

Figure 4. Dispersion of the SPPs in DWCNT: real and imaginary parts of complex propagation constant. Lines 1, 2 and 3 are roots of Eq. (6). Line 4 shows the real part of the propagation constant of SPP in DWCNT without drift current.

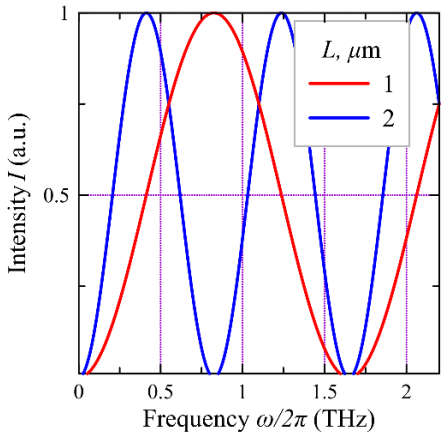

Figure 5. Frequency dependences of the radiation intensity of an array of nanotubes with lengths L = 1 and 2 μm.

The laser-irradiated DWCNTs can be considered as antennas emitting in the THz and far-IR radiation ranges. In the far field region, the angular distribution of the nanotube antenna radiation intensity $I(\theta)$ (θ is the polar angle) at the distance r can be expressed as [36]

$$I(\theta) = \left(\frac{q}{\beta'}\right)^2 \frac{Z\Delta J_{d0}^2}{8\pi^2 r^2} \left[\sin\theta \frac{\cos\left(\frac{qL}{2}\cos\theta\right) - \cos\left(\frac{\beta' L}{2}\right)}{\left(1-\left(q/\beta'\right)^2\cos^2\theta\right)}\right]^2, \quad (7)$$

where $q = \omega/c$ is the wavenumber of radiation from the nanoantenna in the free space, ΔJ_{d0} is the amplitude value of non-stationary current, $Z = 120\pi$ Ohm is the characteristic vacuum impedance. For a given nanotube length L, there is a discrete set of frequencies enabling the formation of standing waves resulting in the intensity given by Eq. (7) reaching a maximum. The maximum condition has the form $\beta' L / 2 = (2m+1)\pi$, (m = 0, 1, 2…), and the minimum length L of the nanotube satisfying the geometric resonance is equal to the SPP wavelength.

Figure 5 shows the frequency dependences of the normalized intensity emitted by the CNT nanoantenna in the transverse direction ($\theta = 90^\circ$) calculated for two fixed values of the length L. It can be seen that to achieve the maximum efficiency of the nanoantenna, it is necessary to tune the SPP frequency. This task is reduced to choosing the radiation frequency of external laser sources. In addition, a corresponding adjustment of the incident angles of laser beams is required in accordance with Figure 3.

CONCLUSIONS

In this work we have proposed a concept of THz generator based on an array of DWCNTs pumped by a direct electric current. The numerical simulations demonstrate the existence of slow SPP modes with a high Q-factor in DWCNTs. We have shown that the electric current can effectively amplify these slow SPP modes. To implement the coherent generation mode at a fixed wavelength, we propose to use coherent excitation of SPPs by two laser beams with slightly different frequencies in the near-IR range. With an array of DWCNTs implementing simultaneous optical irradiation and a drift current, the generation and amplification of SPPs occur at frequencies corresponding to the highest values of the Q-factor. At the same time, the DWCNTs play the role of coherently emitting dipole antennas radiating as a single large dipole. The THz generator proposed in our study could potentially be used in fields demanding a compact source of coherent or at least narrowband THz radiation. These fields include biological and medical research, technical diagnostics, and 6G communication. Plasmonic generators, where the amplification of surface plasmon polaritons (SPPs) is achieved through current pumping, allow for a significantly greater SPP intensity and, consequently, a higher intensity of free THz waves.

ACKNOWLEDGEMENTS

The work was supported by the Russian Science Foundation, grant # 23-19-00880 (the two-beam excitation scheme, DWCNT array dispersion spectra, radiation in the far zone) and grant # 23-79-30017 (the the CNT conductivity model, resonant electric-current-driven amplification of SPPs).

REFERENCES

[1] García-Vidal, F. J., Pitarke, J. M. and Pendry, J. B., “Effective medium theory of the optical properties of aligned Carbon nanotubes,” Phys Rev Lett 78(22), 4289–4292 (1997).

[2] Dai, L., Patil, A., Gong, X., Guo, Z., Liu, L., Liu, Y. and Zhu, D., “Aligned Nanotubes,” ChemPhysChem 4(11), 1150–1169 (2003).

[3] Hao, J. and Hanson, G. W., “Electromagnetic scattering from finite-length metallic carbon nanotubes in the lower IR bands,” Phys Rev B Condens Matter Mater Phys 74(3), 1–6 (2006).

[4] Lidorikis, E. and Ferrari, A. C., “Photonics with multiwall carbon nanotube arrays,” ACS Nano 3(5), 1238–1248 (2009).

[5] Roberts, J. A., Yu, S. J., Ho, P. H., Schoeche, S., Falk, A. L. and Fan, J. A., “Tunable Hyperbolic Metamaterials Based on Self-Assembled Carbon Nanotubes,” rapid-communication, Nano Lett 19(5), 3131–3137 (2019).

[6] Lee, S. B., Teo, K. B. K., Robinson, L. A. W., Teh, A. S., Chhowalla, M., Hasko, D. G., Amaratunga, G. A. J., Milne, W. I. and Ahmed, H., “Characteristics of multiwalled carbon nanotube nanobridges fabricated by poly(methylmethacrylate) suspended dispersion,” Journal of Vacuum Science & Technology B: Microelectronics and Nanometer Structures Processing, Measurement, and Phenomena 20(6), 2773 (2002).

[7] Eletskii, A. V., “Transport properties of carbon nanotubes,” Physics-Uspekhi 52(3), 209 (2009).

[8] Perebeinos, V., Tersoff, J. and Avouris, P., “Electron-phonon interaction and transport in semiconducting carbon nanotubes,” Phys Rev Lett 94(8), 2–5 (2005).

[9] Liu, K., Deslippe, J., Xiao, F., Capaz, R. B., Hong, X., Aloni, S., Zettl, A., Wang, W., Bai, X., Louie, S. G., Wang, E. and Wang, F., "An atlas of carbon nanotube optical transitions," Nat Nanotechnol 7(5), 325–329 (2012).
[10] Slepyan, G. Ya., Maksimenko, S. a., Lakhtakia, A., Yevtushenko, O. and Gusakov, A. V., "Electrodynamics of carbon nanotubes: Dynamic conductivity, impedance boundary conditions, and surface wave propagation," Phys Rev B 60(24), 17136–17149 (1999).
[11] Shuba, M. V., Slepyan, G. Y., Maksimenko, S. A., Thomsen, C. and Lakhtakia, A., "Theory of multiwall carbon nanotubes as waveguides and antennas in the infrared and the visible regimes," Phys Rev B Condens Matter Mater Phys 79(15), 1–17 (2009).
[12] Martín-Moreno, L., De Abajo, F. J. G. and García-Vidal, F. J., "Ultraefficient coupling of a quantum emitter to the tunable guided plasmons of a carbon nanotube," Phys Rev Lett 115(17) (2015).
[13] Kadochkin, A. S., Moiseev, S. G., Svetukhin, V. V., Saurov, A. N. and Zolotovskii, I. O., "Excitation of Ultraslow High-q Surface Plasmon Polariton Modes in Dense Arrays of Double-Walled Carbon Nanotubes," Ann Phys 534(4), 2100438 (2022).
[14] Moradi, A., "Surface Plasmon-Polariton Modes of Metallic Single-Walled Carbon Nanotubes," Photonics Nanostruct 11, 85–88 (2013).
[15] Sharma, S. and Vijay, A., "Terahertz generation via laser coupling to anharmonic carbon nanotube array," Phys Plasmas 25(2) (2018).
[16] Kumar, S., Vij, S., Kant, N. and Thakur, V., "Resonant Terahertz Generation by the Interaction of Laser Beams with Magnetized Anharmonic Carbon Nanotube Array," Plasmonics 17(1), 381–388 (2022).
[17] Kumar, S., Vij, S., Kant, N., Mehta, A. and Thakur, V., "Resonant terahertz generation from laser filaments in the presence of static electric field in a magnetized collisional plasma," The European Physical Journal Plus 136(2), 148 (2021).
[18] Vij, S., Kant, N. and Thakur, V., "Resonant Enhancement of THz Radiation Through Vertically Aligned Carbon Nanotubes Array by Applying Wiggler Magnetic Field," Plasmonics 14(5), 1051–1056 (2019).
[19] Afanas'ev, S. A., Zolotovskii, I. O., Kadochkin, A. S., Moiseev, S. G., Svetukhin, V. V and Pavlov, A. A., "Continuous-wave laser generation of THz slow surface plasmons in an array of single-walled carbon nanotubes," Quantum Electronics 48(9), 849–853 (2018).
[20] Svintsov, D. A., Arsenin, A. V. and Fedyanin, D. Yu., "Full loss compensation in hybrid plasmonic waveguides under electrical pumping," Opt Express 23(15), 19358 (2015).
[21] Moiseev, S. G., Dadoenkova, Y. S., Kadochkin, A. S., Fotiadi, A. A., Svetukhin, V. V. and Zolotovskii, I. O., "Generation of Slow Surface Plasmon Polaritons in a Complex Waveguide Structure with Electric Current Pump," Ann. Phys. 530(11), 1800197 (2018).
[22] Morgado, T. A. and Silveirinha, M. G., "Drift-Induced Unidirectional Graphene Plasmons," ACS Photonics 5(11), 4253–4258 (2018).
[23] Kadochkin, A. S., Moiseev, S., Dadoenkova, Y. S., Bentivegna, F., Svetukhin, V. and Zolotovsky, I. O., "Resonant Amplification of Surface Plasmon Polaritons with an Electric Current in a Single-Walled Carbon Nanotube Lying on a Spatially Modulated Substrate," Journal of Optics 22, 1–7 (2020).
[24] Kadochkin, A. S., Moiseev, S. G., Dadoenkova, Y. S., Svetukhin, V. V. and Zolotovskii, I. O., "Surface plasmon polariton amplification in a single-walled carbon nanotube," Opt Express 25(22), 27165 (2017).
[25] Falkovsky, L. A., "Optical properties of graphene and IV–VI semiconductors," Uspekhi Fizicheskih Nauk 178(9), 923 (2008).
[26] Falkovsky, L. A. and Pershoguba, S. S., "Optical far-infrared properties of a graphene monolayer and multilayer," Phys Rev B Condens Matter Mater Phys 76(15), 153410 (2007).
[27] Yu, P., Fesenko, V. I. and Tuz, V. R., "Dispersion features of complex waves in a graphene-coated semiconductor nanowire," Nanophotonics 7(5), 925–934 (2018).
[28] Nikitin, A. Y., Guinea, F., García-Vidal, F. J. and Martín-Moreno, L., "Edge and waveguide terahertz surface plasmon modes in graphene microribbons," Phys Rev B Condens Matter Mater Phys 84(16), 161407 (2011).
[29] Hajaj, E. M., Shtempluk, O., Kochetkov, V., Razin, A. and Yaish, Y. E., "Chemical potential of inhomogeneous single-layer graphene," Phys Rev B Condens Matter Mater Phys 88(4) (2013).
[30] Fateev, D. V. and Popov, V. V., "Hydrodynamic Terahertz Plasmons and Electron Sound in Graphene with Spatial Dispersion," Semiconductors 54(8), 941–945 (2020).
[31] Tsimring S. E., Electron Beams and Microwave Vacuum Electronics, John Wiley & Sons, Inc., Hoboken, NJ, USA (2006).

[32] Abramov, A. S., Zolotovskii, I. O., Moiseev, S. G., Sementsov, D. I., “Amplification and generation of surface plasmon polaritons in a semiconductor film–dielectric structure,” Quantum Electronics 48(1), 22–28 (2018).
[33] Zolotovskii, I. O., Dadoenkova, Y. S., Moiseev, S. G., Kadochkin, A. S., Svetukhin, V. V and Fotiadi, A. A., “Plasmon-polariton distributed-feedback laser pumped by a fast drift current in graphene,” Phys. Rev. A 97, 053828 (2018).
[34] Zolotovskii, I. O., Dadoenkova, Y. S., Bentivegna, F. F. L., Kadochkin, A. S., Moiseev, S. G., Svetukhin, V. V., “Resonant amplification of slow surface plasmon polaritons in a DC current pumped semiconductor/graphene waveguide with a groove defect,” Optics & Laser Technology 166, 109593 (2023).
[35] Branch, G. M. and Mihran, T. G., “Plasma Frequency Reduction Factors in Electron Beams,” IRE Transactions on Electron Devices 2(2), 3–11 (1955).
[36] Burke, P. J., Shengdong Li and Zhen Yu., “Quantitative theory of nanowire and nanotube antenna performance,” IEEE Trans Nanotechnol 5(4), 314–334 (2006).